Tabletop soft-x-ray Fourier transform holography with 50 nm resolution

R. L. Sandberg,[1,*] D. A. Raymondson,[1] C. La-o-vorakiat,[1] A. Paul,[1] K. S. Raines,[2] J. Miao,[2] M. M. Murnane,[1] H. C. Kapteyn,[1] and W. F. Schlotter[3,4]

[1]*Deparment of Physics and JILA, University of Colorado at Boulder and National Institute of Standards and Technology, Boulder, Colorado 80309-0440, USA*
[2]*Department of Physics and Astronomy and California NanoSystems Institute, University of California, Los Angeles, California 90095, USA*
[3]*Stanford Synchrotron Radiation Laboratory, SLAC National Accelerator Laboratory, Menlo Park, California 94025, USA*
[4]*Institute for Experimental Physics, University of Hamburg, Luruper Chausee 149, 22761 Hamburg, Germany*
*Corresponding author: richard.sandberg@colorado.edu

We present what we believe to be the first implementation of Fourier transform (FT) holography using a tabletop coherent x-ray source. By applying curvature correction to compensate for the large angles inherent in high-NA coherent imaging, we achieve image resolution of 89 nm using high-harmonic beams at a wavelength of 29 nm. Moreover, by combining holography with iterative phase retrieval, we improve the image resolution to <53 nm. We also demonstrate that FT holography can be used effectively with short exposure times of 30 s. This technique will enable biological and materials microscopy with simultaneously high spatial and temporal resolution on a tabletop soft-x-ray source. © 2009 Optical Society of America

OCIS codes: 090.4220, 100.5070, 110.1650, 340.7440, 340.7480.

Microscopy is a critical enabling tool for understanding the nano world. By virtue of its short wavelength, soft-x-ray (SXR) microscopy has revealed nanometer-scale resolution images of whole unstained cells, magnetic permalloy wires, internal structures in nanocrystals, and magnetic domains in thin film samples [1,2]. Recent developments promise to open up soft x-ray microscopy for more widespread use. First, new diffractive imaging techniques using coherent x-ray beams have made possible nanometer-scale resolution imaging by essentially replacing the imaging optics in a microscope with an oversampling iterative phase-retrieval algorithm [1–6]. Second, advances in coherent SXR generation using ultrafast lasers have begun to provide sufficient coherent flux for tabletop SXR imaging [7–10]. In past work we demonstrated coherent diffractive imaging with iterative phase retrieval using two coherent tabletop SXR sources. Image resolutions of 94 nm were obtained using 29 nm light produced by a high-harmonic source, while resolutions of 71 nm were obtained using a 46.9 nm SXR laser [11,12].

Fourier transform (FT) holography is a coherent diffractive imaging technique that is complementary to iterative phase retrieval and well suited for tabletop sources with limited flux. In FT holography, an unknown sample object and a known reference structure are illuminated with a single coherent beam. Interference between the scattered light from the reference and the object are detected in the far field as a Fourier transform hologram [13–15]. A two-dimensional (2D) image of the sample is then easily reconstructed by computing the magnitude of the 2D Fourier transformation of the detected hologram, which gives the spatial autocorrelation of the sample. For each reference hole, a cross correlation of the sample and a reference hole produces a subimage and its complex conjugate. To obtain the highest possible image resolution, the reference beam should diverge very strongly, thus requiring a small reference source size located in the same plane as the sample. To increase the signal-to-noise ratio of images produced using FT holography, multiple reference beams can be used [15]. The multiple subimages produced can then be averaged to improve the image quality.

In this work, we combine two coherent diffractive imaging techniques, multiple reference FT holography and oversampling phase retrieval, to achieve what we believe are the highest spatial resolution images (<53 nm) demonstrated to date using high harmonics. Furthermore, we demonstrate high-resolution imaging (125 nm) with exposure times that are suitable for practical applications (30 s). This represents a significant improvement over past work, where exposure times of greater than 1 h were required for comparable image quality.

The schematic of the experimental setup is shown in Fig. 1. A coherent beam from a tabletop high-harmonic source is focused onto a multiple reference FT holography sample, and the coherent diffraction pattern, or the hologram, is detected in the far field on a CCD. To generate the 29 nm high-harmonic generation (HHG) beam, 1.3 mJ, 25 fs laser pulses from a 4 W, 3 kHz Ti:sapphire laser are focused into an argon-filled hollow waveguide with an inner diameter of 150 μm. When the argon pressure inside the waveguide is ~70 Torr, the HHG process is phase matched, resulting in a bright, highly Gaussian, narrowband SXR beam with divergence <1 mrad. A pair of Si/Mb multilayer mirrors with a bandwidth of 2.5 nm (one flat and one 50 cm radius of curvature) are used to select a single harmonic at 29 nm and to focus it onto the sample. After reflecting from these mirrors, the selected harmonic beam has a narrow
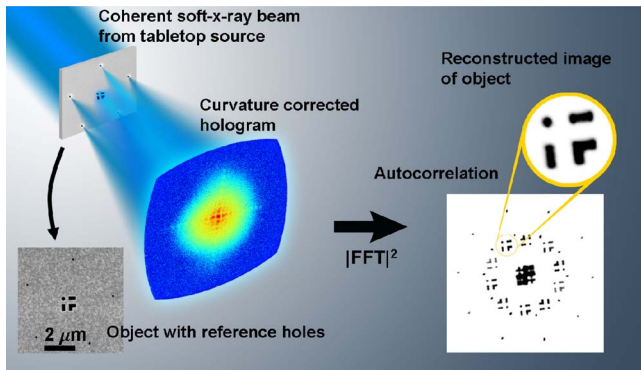
Fig. 1.   (Color online) Multiple reference FT holography. A coherent high-harmonic beam with $\lambda = 29$ nm illuminates a test pattern surrounded by five reference holes. The scattered light interferes and is recorded on a CCD camera in the far field as a hologram (log scale). The spatial autocorrelation of the object can be retrieved by taking the squared magnitude of the Fourier transform of the hologram. A single subimage from the autocorrelation is shown.

bandwidth of $\lambda / \Delta\lambda > 250$, giving a longitudinal coherence $\xi_1 = \lambda^2 / \Delta\lambda > 7.3$ μm. The spot size on the sample is ~ 20 μm, with an average photon flux of $\sim 2 \times 10^8$ photons per second. The sample is held on an x–y piezo actuated stage, placed 17 mm from a backthinned CCD. The test object consists of a central pattern surrounded by five fully transmissive reference holes of $\sim 125 \pm 6$ nm diameter, as shown in Fig. 1. The sample was created by focused ion beam milling of a 100-nm-thick silicon nitride window, coated with 400 nm of gold. The reference holes were milled all the way through the sample, while the nitride was left on the central test pattern.

Figure 2 summarizes our experimental results using FT holography alone. Figure 2(a) shows a logarithmic, curvature corrected, hologram of the sample shown in Fig. 1. There is only 17 mm between the sample and the center of the detector (momentum transfer of $q = 0$). Nevertheless, signal can be detected above the noise more than 700 pixels away from the center ($q = 4\pi \sin \theta / \lambda = \pm 0.211$ nm^{-1}). Such a large NA (NA = 0.5) violates the paraxial approximation, because the wavefront originating at the sample will be significantly distorted at high angles when recorded on a flat detector. Correction of these distortions is accomplished by mapping the flat hologram onto a spherical surface, thus accounting for distortions such as pixel skew and stretching at higher angles [12].

The hologram in Fig. 2(a) is a summation of eight separate 600 s exposures. The background is first subtracted from the data, then cosmic rays are removed, followed by summing of the separate exposures. Next, a curvature correction is applied to the summed data, and a Gaussian filter is applied to the hard edge of the curvature corrected data. One of the five subimages from the autocorrelation shown in Fig. 1 is enlarged in Fig. 2(b), showing a resolution of 89 nm. The fundamental resolution limit for this geometry where the object is convolved with a circular reference is $\sim 70\%$ of the diameter of the 125 nm ref-
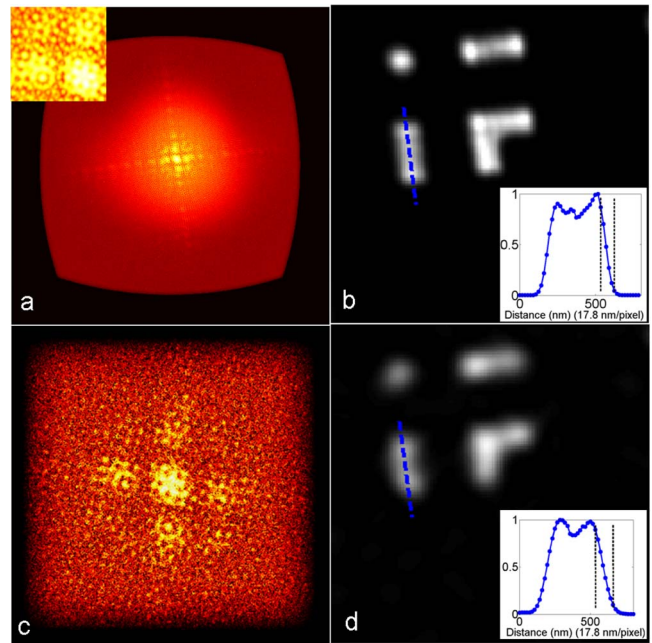

Fig. 2.   (Color online) (a) Curvature corrected hologram from a composite 4800 s exposure ($q_{max} = \pm 0.211$ nm^{-1}). The inset shows the detail of the center of the diffraction pattern. (b) Single subimage reconstruction with a lineout (inset) demonstrates 89 nm resolution (17.8 nm per pixel). (c) Hologram recorded from 30 s of exposure ($q_{max} = \pm 0.045$ nm^{-1}). (d) Single subimage reconstruction for a 30 s exposure (17.8 nm per pixel), showing a lineout (blue dashed line) demonstrating 125 nm resolution (inset).

erence holes, or ~ 88 nm [16]. Thus, we achieve the theoretically limited resolution.

Moderately high-resolution image resolutions can be achieved after only 30 s of exposure. Figure 2(c) shows the hologram recorded with a 30 s exposure, containing approximately 15,000 detected 29 nm photons. Figure 2(d) shows one subimage from this short-exposure data. A lineout along the dashed line gives a resolution of 125 nm, as shown in the inset.

Significantly enhanced resolution can be achieved by applying an iterative phase retrieval algorithm to the oversampled hologram recorded using longer exposures [5,14,17,18]. The only input necessary for this hybrid approach is the previously recorded hologram. In real space, the resolution of the FT holographic image reconstruction is limited by the size of the reference hole. If light scattered from the unknown object extends beyond the Airy disk of the reference holes, then higher spatial frequency information about the unknown object is recorded in the hologram, although it cannot be accessed using the Fourier transform reconstruction alone. We used the guided hybrid input-output algorithm for this reconstruction with 16 independent reconstructions, 8 generations with 2000 iterations per generation, and we averaged the 5 best independent reconstructions in the final image [19].

Figure 3 summarizes the results of performing phase retrieval on the measured hologram [1,19]. Figure 3(a) shows a magnified scanning electron microscope (SEM) image of the sample. Figure 3(b) shows the curvature-corrected hologram from a com-
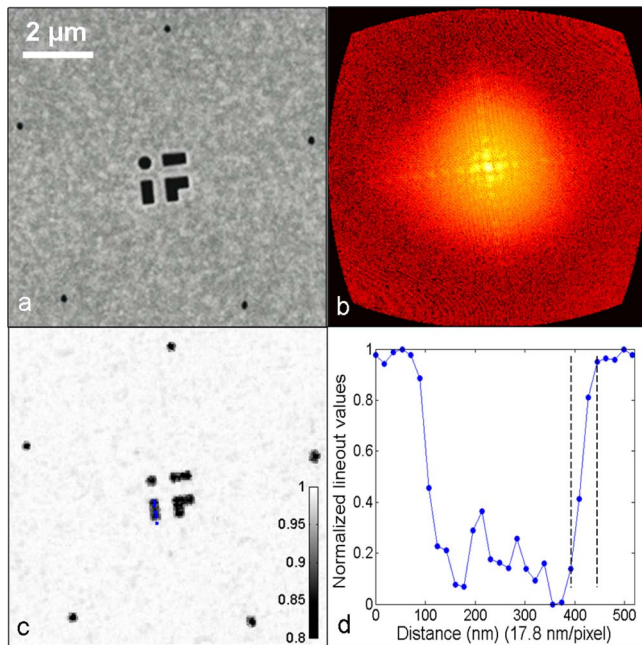
Fig. 3. (Color online) (a) SEM image of the sample. (b) Log of the curvature corrected hologram used in the iterative phase retrieval ($q_{max} = \pm 0.211$ nm^{-1}). (c) Reconstructed image of the sample using a phase-retrieval algorithm to refine the resolution to 53 nm (17.8 nm per pixel), as demonstrated in the lineout (dotted line) shown in (d).

posite 4800 s exposure. Figure 3(c) shows the final reconstructed 2D image of the sample, demonstrating a resolution of 53 nm, as shown by the lineout along the dashed line [shown in Fig. 3(d)].

This hybrid holography/phase retrieval technique has several notable advantages. First, while image recovery using phase retrieval takes hours of processor time, reconstruction using the FT holography method takes only seconds. Thus the hybrid holographic/phase retrieval technique allows for quick feedback regarding low-resolution features of a sample. Significant improvements in resolution are then possible by applying phase-retrieval techniques to the hologram, within the limits set by the wavelength, NA, and signal-to-noise ratio. Also, the reference holes in FT holography break the symmetry of the sample, resulting in quicker convergence in the phase-retrieval algorithm [17,18]. This hybrid approach also eases the requirement for pointlike reference features that are difficult to manufacture.

In conclusion, we have introduced a practical, tabletop, diffractive SXR microscopy system capable of fast-feedback moderate-resolution imaging (sub-100 nm) using FT holography. In combination with oversampling phase retrieval algorithms, very high image resolutions of 53 nm can be achieved, which to our knowledge are the highest resolution images demonstrated to date using high-harmonic sources. In the future, new phase-matching schemes promise to increase the high-harmonic flux at shorter wavelengths relevant to biological and materials imaging [20,21].

References

1. C. Song, H. Jiang, A. Mancuso, B. Amirbekian, L. Peng, R. Sun, S. S. Shah, Z. H. Zhou, T. Ishikawa, and J. Miao, Phys. Rev. Lett. **101**, 158101 (2008).
2. S. Eisebitt, J. Lüning, W. F. Schlotter, M. Lörgen, O. Hellwig, W. Eberhardt, and J. Stöhr, Nature **432**, 885 (2004).
3. J. Miao, P. Charalambous, J. Kirz, and D. Sayre, Nature **400**, 342 (1999).
4. S. Marchesini, H. He, H. N. Chapman, S. P. Hau-Riege, A. Noy, M. R. Howells, U. Weierstall, and J. C. H. Spence, Phys. Rev. B **68**, 140101 (2003).
5. B. Abbey, K. A. Nugent, G. J. Williams, J. N. Clark, A. G. Peele, M. A. Pfeifer, M. de Jonge, and I. McNulty, Nat. Phys. **4**, 394 (2008).
6. P. Thibault, M. Dierolf, A. Menzel, O. Bunk, C. David, and F. Pfeiffer, Science **321**, 379 (2008).
7. R. A. Bartels, A. Paul, H. Green, H. C. Kapteyn, M. M. Murnane, S. Backus, I. P. Christov, Y. Liu, D. Attwood, and C. Jacobsen, Science **297**, 376 (2002).
8. M. Wieland, C. Spielmann, U. Kleineberg, T. Westerwalbesloh, U. Heinzmann, and T. Wilhein, Ultramicroscopy **102**, 93 (2005).
9. P. W. Wachulak, R. A. Bartels, M. C. Marconi, C. S. Menoni, J. J. Rocca, Y. Lu, and B. Parkinson, Opt. Express **14**, 9636 (2006).
10. Y. Wang, E. Granados, F. Pedaci, D. Alessi, B. Luther, M. Berrill, and J. J. Rocca, Nat. Photonics **2**, 94 (2008).
11. R. L. Sandberg, A. Paul, D. A. Raymondson, S. Hadrich, D. M. Gaudiosi, J. Holtsnider, R. I. Tobey, O. Cohen, M. M. Murnane, H. C. Kapteyn, C. Song, J. Miao, Y. Liu, and F. Salmassi, Phys. Rev. Lett. **99**, 098103 (2007).
12. R. L. Sandberg, C. Song, P. W. Wachulak, D. A. Raymondson, A. Paul, B. Amirbekian, E. Lee, A. E. Sakdinawat, O. V. C. La, M. C. Marconi, C. S. Menoni, M. M. Murnane, J. J. Rocca, H. C. Kapteyn, and J. Miao, Proc. Natl. Acad. Sci. USA **105**, 24 (2008).
13. I. McNulty, J. Kirz, C. Jacobsen, E. H. Anderson, M. R. Howells, and D. P. Kern, Science **256**, 1009 (1992).
14. S. Eisebitt, M. Lörgen, W. Eberhardt, J. Lüning, S. Andrews, and J. Stöhr, Appl. Phys. Lett. **84**, 3373 (2004).
15. W. F. Schlotter, R. Rick, K. Chen, A. Scherz, J. Stohr, J. Luning, S. Eisebitt, C. Gunther, W. Eberhardt, O. Hellwig, and I. McNulty, Appl. Phys. Lett. **89**, 163112 (2006).
16. W. F. Schlotter, Ph.D. dissertation (Stanford University, 2007).
17. S. Marchesini, A. E. Sakdinawat, M. J. Bogan, A. Barty, H. N. Chapman, M. Frank, S. P. Hau-Riege, A. Sz, C. Cui, and D. A. Shapiro, Nat. Photonics **2**, 560 (2008).
18. L. M. Stadler, C. Gutt, T. Autenrieth, O. Leupold, S. Rehbein, Y. Chushkin, and G. Grübel, Phys. Rev. Lett. **100**, 245503 (2008).
19. C. C. Chen, J. Miao, C. W. Wang, and T. K. Lee, Phys. Rev. B **76**, 064113 (2007).
20. H. Kapteyn, O. Cohen, I. Christov, and M. Murnane, Science **317**, 775 (2007).
21. T. Popmintchev, M.-C. Chen, O. Cohen, M. E. Grisham, J. J. Rocca, M. M. Murnane, and H. C. Kapteyn, Opt. Lett. **33**, 2128 (2008).